

Effect of the liquid temperature on the interaction behavior for single water droplet impacting on the immiscible liquid

Tiantian Wang(汪甜甜), Changjian Wang(王昌建), Shengchao Rui(芮圣超), and Kai Pan(泮凯)
Citation: Chin. Phys. B, 2021, 30 (**11**): 116801. DOI: 10.1088/1674-1056/abf34b
Journal homepage: http://cpb.iphy.ac.cn; http://iopscience.iop.org/cpb

What follows is a list of articles you may be interested in

Dielectrowetting actuation of droplet: Theory and experimental validation

Yayan Huang(黄亚俨), Rui Zhao(赵瑞), Zhongcheng Liang(梁忠诚), Yue Zhang(张月), Meimei Kong(孔梅梅), and Tao Chen(陈陶)
Chin. Phys. B, 2021, 30 (**10**): 106801. DOI: 10.1088/1674-1056/ac1926

Continuous droplet rebound on heated surfaces and its effects on heat transfer property: A lattice Boltzmann study

Qing-Yu Zhang(张庆宇), Qi-Peng Dong(董其鹏), Shan-Lin Wang(王山林), Zhi-Jun Wang(王志军), and Jian Zhou(周健)
Chin. Phys. B, 2021, 30 (**4**): 044703. DOI: 10.1088/1674-1056/abd745

Droplets breakup via a splitting microchannel

Wei Gao(高崴), Cheng Yu(于程), Feng Yao(姚峰)
Chin. Phys. B, 2020, 29 (**5**): 054702. DOI: 10.1088/1674-1056/ab7b4b

Effects of square micro-pillar array porosity on the liquid motion of near surface layer

Xiaoxi Qiao(乔小溪), Xiangjun Zhang(张向军), Ping Chen(陈平), Yu Tian(田煜), Yonggang Meng(孟永钢)
Chin. Phys. B, 2020, 29 (**2**): 024702. DOI: 10.1088/1674-1056/ab5fba

Measurement of the friction coefficient of a fluctuating contact line using an AFM-based dual-mode mechanical resonator

Guo Shuo, Xiong Xiao-Min, Xu Zu-Li, Shen Ping, Tong Penger
Chin. Phys. B, 2014, 23 (**11**): 116802. DOI: 10.1088/1674-1056/23/11/116802

Effect of the liquid temperature on the interaction behavior for single water droplet impacting on the immiscible liquid*

Tiantian Wang(汪甜甜)[1,2], Changjian Wang(王昌建)[1,3,†], Shengchao Rui(芮圣超)[1,2], and Kai Pan(泮凯)[1]

[1] *School of Civil Engineering, Hefei University of Technology, Hefei* 230009, *China*
[2] *Anhui International Joint Research Center on Hydrogen Safety, Hefei* 230009, *China*
[3] *Engineering Research Center of Safety Critical Industrial Measurement and Control Technology, Ministry of Education, Hefei* 230009, *China*

(Received 7 February 2021; revised manuscript received 17 March 2021; accepted manuscript online 30 March 2021)

The interaction of single water droplet impacting on immiscible liquid surface was focused with the temperature varying from 50 °C to 210 °C. The impact behavior is recorded with a high-speed camera running at 2000 frames per second. It is found that droplet diameter, oil temperature, and Weber number have important influences on impact behaviors. Three typical phenomena, including penetration, crater-jet, and crater-jet–secondary jet, were observed. Penetration only occurs when the Weber number is below 105. With Weber number increasing to 302, the jet begins to appear. Moreover, to gain deeper physical insight into the crater formation and jet formation, the energy of droplet impingement onto the liquid pool surface was estimated. The oil temperature has a significant effect on the energy conversion efficiency. High temperature is beneficial to improve energy conversion efficiency.

Keywords: droplet impact, crater-jet, weber number, immiscible liquid

PACS: 68.05.–n, 47.55.dr, 47.55.db **DOI:** 10.1088/1674-1056/abf34b

1. Introduction

The interaction between a single droplet and solid surface or liquid surface has attracted more research attentions,[1–14] such as spray cooling,[15] inkjet printing,[16] water spray extinguishing,[17,18] and enhanced heat transfer, *etc.* Droplet impacts were first studied by Worthington[19] over one hundred years ago. Droplet-surface interactions are mainly focused on liquid–liquid and liquid–solid interactions. Previous studies have found some interesting phenomena, including bounce, jet, and surface bubble[20–22] when the droplets impact on the liquid surface. The impact phenomena are mainly affected by the physical and chemical properties of the impinged liquid, the impact Weber number, the temperature of the oil pool, the depth of the oil pool, and so on.

Liang *et al.*[23–25] systematically investigated the impact behaviors of a single water droplet impacting on inclined solid surfaces with the thin liquid film. They pointed out that water droplet surface tension, viscosity, and the impact angle affected the impact behavior of droplets on sloping wet surfaces or wet cylindrical surfaces. Zou *et al.*[26,27] studied the phenomenon of water droplets impacting on the surface of restricted liquid, and found that with the increase in Weber number, water droplets could be observed to float, jump, condense, and splash. Fan *et al.*[28] carried out the experiments on the single droplet impacting on heptane pool with the dimensionless depth from 1.8 to 10.8, and pointed out that there is a clear correlation between the impact behavior and the depth of the liquid pool. Penetration occurred when the dimensionless depth of less than 3.6, and crater-jet–secondary jet just could be seen when the dimensionless depth exceeded 5.4. Hasegawa *et al.*[29] studied three kinds of single droplets with different densities, viscosities, and surface tensions to impact the liquid pool. They found that the observed impact phenomenon was affected by the impact velocity. In the estimation of the energy balance of the water drop impacting on the surface of the liquid pool, it is found that regardless of the nature of the liquid, about 28% of the impact energy is used for the formation of the cavity. The remaining energy is likely to be dissipated or consumed on the surface.

However, most of the above studies are carried out at room temperature, mainly focusing on the effects of different types of fuel, pool depth, and impact velocity, *etc.* At present, some studies are mainly focused on a single droplet impacting on the hot surface from the fire suppression perspective. Typically, Xu *et al.*[30] investigated the impact of water droplet on the burning ethanol oil pool, discussed in detail the critical conditions for the occurrence of three typical phenomena: crater-jet, crater-jet–secondary jet, and surface bubble, and derived the theoretical values of the central jet length scale and maximum crater depth from energy conservation.

Although the impact behavior of single droplet onto miscible liquid has been extensively studied,[26,28,30–32] the behavior and mechanism of droplet interaction with the immiscible

*Project supported by the National Key Research and Development Program of China (Grant No. 2017YFC0805100) and the Fundamental Research Funds for the Central Universities of China (Grant No. PA2020GDGP0052).

†Corresponding author. E-mail: chjwang@hfut.edu.cn

© 2021 Chinese Physical Society and IOP Publishing Ltd

liquid is still unclear, and especially the effect of oil pool temperature on the impact characteristic parameters have not been clarified. For obtaining insight into the interaction between water droplet and liquid surface at various temperatures and the fire extinguishing mechanism of water spray, high viscosity engine oil was used as the fuel in experiment. Engine oil is widely used in industry, and its viscosity, density, and surface tension changes with the temperature, which affects the performance of engine oil. A series of the experiments was carried out on the impact of a single water drop on the heat engine oil pool, and the impact behavior was analyzed and the related parameters were discussed.

2. Experimental setup

The experiment system is demonstrated in Fig. 1. The main components include an image acquisition device, a water droplet generator, a temperature collecting device, a heating plate and an oil pool. The droplet generator was composed of injection pump syringes and needles in a steady injection rate of 0.1 ml/h of the injection pump. The small droplet formed slowly at the needle tip and then the droplet was free to fall under its own gravity. In order to eliminate the contamination of the oil pool by falling water, the oil is replaced after each impact. The whole impact behaviors were recorded by an NAC high-speed photography camera with 2000 FPS, equipped with a 100-mm Tokina macro lens. According to the time-dependent images in each test, the drop diameter D and impact velocity v were determined by image processing. To acquire the droplet diameter and other parameters, pixel analyzing was conducted with the software Photoshop CC 2018 and a reference ruler. The error is 1 pixel with size of 0.082 mm. The light source was provided by a 1000-W halogen lamp. The temperature distributions of the oil pool were measured by the K-type thermocouples with an accuracy ± 1 °C. Four K-type thermocouples were located at 1 mm, 17 mm, 33 mm, and 49 mm beneath the oil surface to monitor the temperature. It can be seen from the temperature profile with time that, from the bottom of the pool to the liquid surface, the temperature varied with about 2 ± 0.5 °C. The pool bottom temperature is slightly higher than the liquid surface temperature. A heater plate, which could adjust the oil temperature ranging from 20 °C to 600 °C, was used to heat the engine oil to a target temperature. The liquid pool was made of transparent quartz glass resistant high temperature with a thickness of 2 mm and a length, width and height of 75 mm, 75 mm, and 80 mm. In this study, the great wall brand engine oil was used as the impacted liquid while pure water was used as droplets. Tables 1 and 2 show the liquid properties. The water droplet that formed at the needle is still approximately spherical under the gravity effect. Similar to previous studies,[33,34] the mean drop diameter is determined by image and can be expressed as $D = \left(D_x^2 D_y\right)^{1/3}$, where D_x and D_y represent the horizontal and vertical diameters. By changing the needle diameter, the water droplet diameter D was varied between 2.8 nm and 4.5 mm, with a measuring error of ± 0.1 mm. Meanwhile, by adjusting the impact height h between the needle tip and the engine oil level was changed from 10 cm to 90 cm, the impact velocity v was varied between 1.24 m/s and 4.16 m/s, with an accuracy of ± 0.05 m/s. The thickness of the liquid pool was fixed at 50 mm, so as to avoid interference from the pool and container wall. The Weber number can be expressed as $We = (D/\sigma)\rho v^2$, where D, σ, ρ, v are the initial diameter, surface tension, density, and velocity of water droplet, respectively.

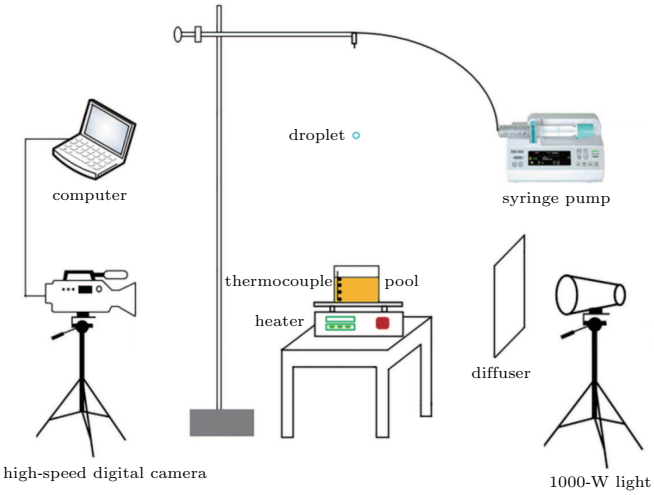


Fig. 1. Schematic diagram of experimental apparatus.

Table 1. Physics properties of engine oil.

Physics properties	50 °C	70 °C	90 °C	110 °C	130 °C	170 °C	210 °C
Density (kg/m^3)	854.5	837.1	819.2	811.0	791.7	751.3	723.4
Surface tension (mN/m)	26.9	24.9	22.8	19.7	19.3	16.2	14
Viscosity (mPa·s)	120.9	42.3	9.2	6.9	5.1	3.6	1.8

Table 2. Physical properties of water ($T = 20$ °C).

Fluid	Density (kg/m^3)	Surface tension (mN/m)	Viscosity (mPa·s)	Boiling temperature (°C)
Distilled water	997	72	1.002	100

3. Results and discussion

3.1. Impact behaviors

In experiment, the research focused on the effects of different temperatures of hot engine oil on the droplet impact behaviors. The oil temperature ranges from 50 °C to 210 °C, and resultantly three kinds of typical phenomena can be observed, including penetration, crater-jet, and crater-jet–secondary jet.

Figure 2(a) shows the behaviors of the single water droplet impacting on the hot engine oil surface with the temperature of 50 °C and $We = 105$. Time $t = 0$ is the moment of droplet impingement on the oil surface. Because of the droplet with high velocity impacting on the oil surface, an obvious crater structure is formed on the surface of the oil pool at 9 ms. At 20 ms, the crater continues to expand outward until the crater structure reaches its maximum depth. At 35 ms, the unbroken droplet passes through the crater with the help of its kinetic energy and then continues to move downwards. Finally, it sticks to the bottom of the pool, no splash, crown and jet structure appear in the whole process. The whole behavior is called the penetration.

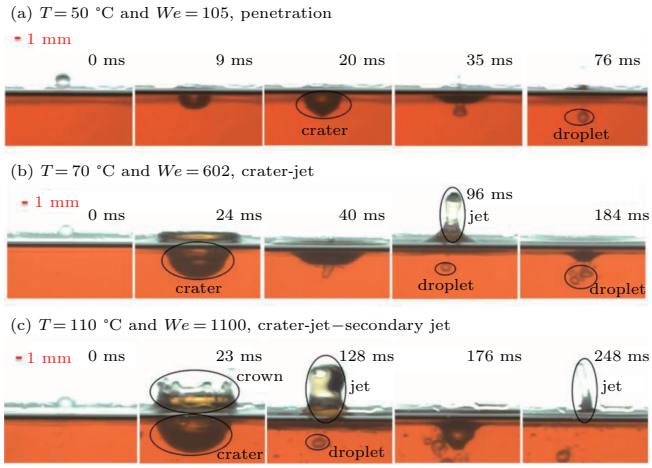


Fig. 2. Impact behavior evolution processes for single water droplet impacting on hot engine oil surface: (a) $T = 50$ °C, $We = 105$; (b) $T = 70$ °C, $We = 603$; (c) $T = 110$ °C, $We = 1100$.

Figure 2(b) shows the behavior of the single water droplet impacting on a hot engine oil surface with the temperature of 70 °C and $We = 603$. At 24 ms, the largest crater structure is formed. Subsequently, the engine oil around the crater wall begins to flow inward, filling the crater, and then a jet rises from the oil surface. At 96 ms, the jet structure with the maximum height is formed. Then, the liquid column collapses and the jet completely disappears at 184 ms. The whole behavior is called the crater-jet. Compared with the single droplet impacting miscible ethanol pool,[35] a significant difference can be found. The time when the droplet impacts the ethanol surface to observe the largest crater and the largest jet structure is earlier than that of the impact on the engine oil surface. Moreover, it is difficult to observe the complete sub-droplet falling in the ethanol pool after the impact.

Figure 2(c) shows the behavior of the single water droplet impacting on a hot engine oil surface with the temperature of 110 °C and $We = 1100$. At 23 ms, a crown structure is formed on the liquid surface. Subsequently, the crown structure collapses under its own gravity. At 128 ms, an obvious jet structure can be observed. Then, the jet breaks up, and it should be mentioned that the energy of the first jet is not dissipated completely after the droplet falls into the oil pool, so the second jet is generated above the liquid level of the oil pool. At 248 ms, the secondary jet reaches its maximum height. The whole behavior is called the crater-jet–secondary jet. The maximum volume of the secondary jet is obviously smaller than that of the primary jet. In current study, all the studies on jet parameters are represented by the primary jet.

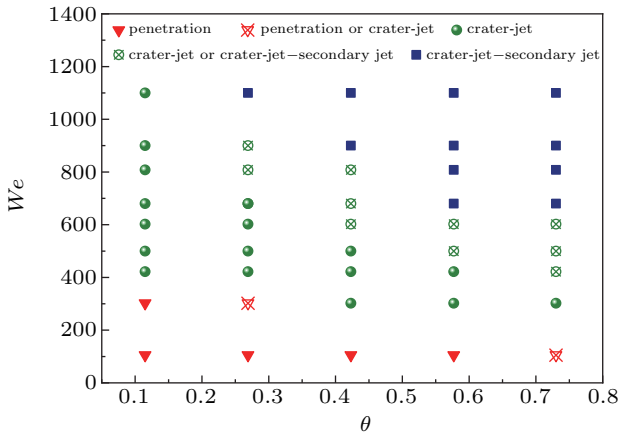


Fig. 3. Phase diagram of impact phenomena.

Figure 3 shows the regime diagram of impact phenomena. Each case was repeated 10 times. The non-dimensional pool temperature can be expressed as $\theta = (T - T_\infty)/(T_{\text{boiling}} - T_\infty)$ ($T_\infty = 20$ °C, $T_{\text{boiling}} = 280$ °C). The penetration phenomenon can be observed for low Weber number because the initial impact energy is small enough and the impact force is very small when the water droplet reaches the liquid level, so it is difficult to have enough energy to support the oil surface deformation and form a complete crater jet structure. For the two transition regions, repeated experimental data show that the two phenomena involved in the transition region occur randomly. For the crater-jet phenomenon, it is seen that the critical impact Weber number of crater-jet decreases with the increase of oil temperature. This agrees with the results of Manzello *et al.*[36] The jet can be found when the Weber number exceeds 302. For crater-jet–secondary jet, it is easier to form a secondary jet for high Weber number and high temperature. Many previous studies[31,37] found the surface bubble phenomenon when the Weber number was increased to a certain critical value. At the same time, Xu *et al.*[38] reported that the increase in the temperature of the impacted oil pool is beneficial to the formation of the surface bubble. When the Weber number exceeds

530, the surface bubble phenomenon can be observed when the droplet impacts the ethanol liquid. However, in this work, no surface bubbles were found.

3.2. Maximum crater volume and maximum jet height

According to Ref. [29], the crater is hemispherical and its volume can be expressed as: $V_c = (2/3)\pi R^2 H_d$, where R is the radius of the crater and H_d is the depth of the crater. The crater is formed after the droplet touches the oil surface, and the crater volume reaches the maximum at about 50 ms. Figure 4 presents the crater volume for different oil pool temperatures. Error bars denote the standard deviation of each set of data. When the oil temperature is 210 °C, the crater volume growth rate is faster than when the oil temperature is 90 °C, indicating a clear correlation between the cavity volume growth rate and the oil temperature. The temperature of the oil affects the maximum crater volume, and the increase of oil temperature is beneficial to the increase of crater volume. The evolution process from the droplet contacting the liquid surface to the formation of the maximum crater volume is about 24 ms–27 ms. With the temperature of the oil pool from 90 °C to 210 °C, the physical properties of the oil (such as viscosity, surface tension, density, *etc.*) have changed greatly. It is obviously found that the formation time of the largest crater remains nearly constant with the increase of oil temperature, which means that the physical properties of the oil have little effect on the formation time of the largest crater. Gray solid points and green solid points respectively plot the time evolution of water droplet and ethanol droplet impinging on the water surface. Hasegawaa *et al.*[29] reported that the time for the water and ethanol droplet to form the maximum crater volume when it impacts the water surface is about 14 ms–18 ms, which was far less than the time for a droplet to hit the surface of oil. So the immiscibility of water and oil has an important influence on the impact process.

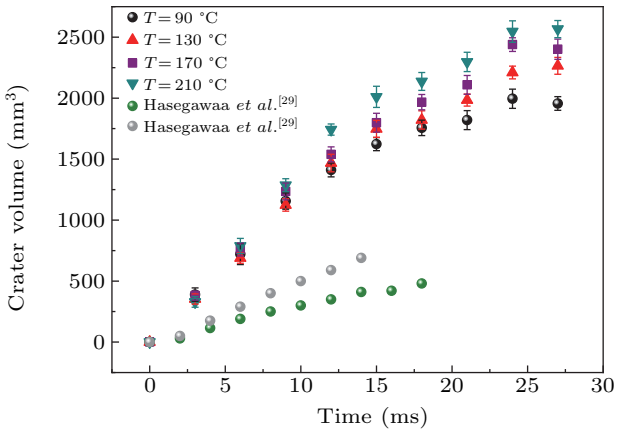


Fig. 4. Temporal evolution of cavity volumes of water with different oil temperatures.

Figure 5 shows the influence of various droplet diameters on the maximum crater volume. The increase of droplet diameter induces the increase of the maximum crater volume. This implies that both the droplet diameter and the temperature of the oil pool influence the volume of the crater. The larger the droplet diameter is, the greater the initial kinetic energy is, and resultantly the more energy can be provided to form the crater. Furthermore, for the same droplet diameter, maximum volume increases with the temperature of the oil pool from 90 °C to 210 °C. The physical properties of fuel have an important effect on the formation of craters. As the oil temperature increases, the viscosity, surface tension, and density of the fuel all decrease, so that when a single droplet impacts onto target liquid surface, the flow resistance is reduced, and the droplet easily penetrates the target liquid.

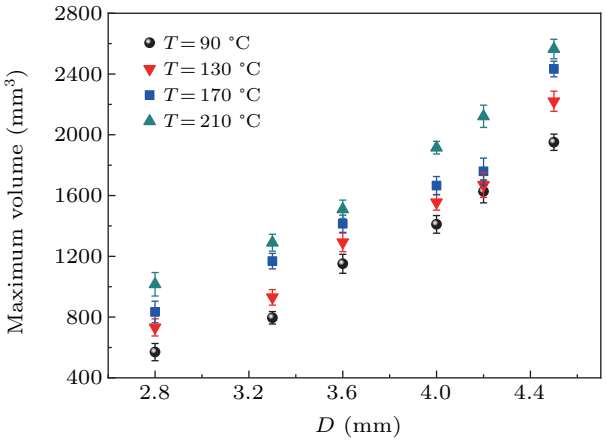


Fig. 5. Maximum volume of the crater as a function of droplet diameters.

Figure 6 shows the relationship between the maximum jet height and the impact Weber number. It was obviously observed that, when the Weber number varies from 105 to 1100, the maximum jet height increases rapidly with the Weber number. The observed impact phenomenon is crater-jet. For the same Weber number, the increase in oil temperature can lead to an increase of the maximum jet height. When the Weber number is increased to 808, the impact phenomena at the oil temperature of 110 °C and 130 °C turn into the crater-jet–secondary jet, and the maximum jet height continues to increase.

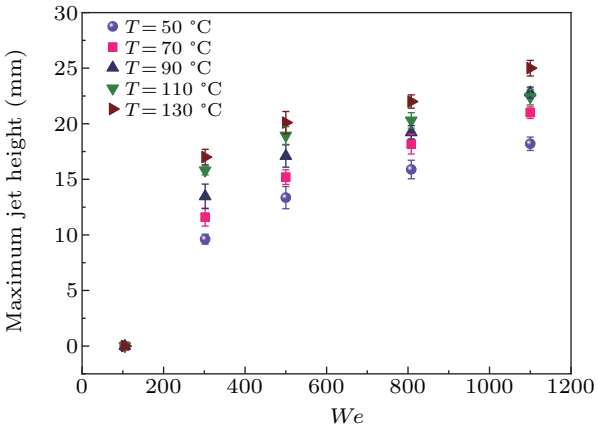


Fig. 6. Maximum height of the jet as a function of Weber number.

3.3. Energy conversion and conservation

When the water droplets reach the surface of the oil, the oil near the impact point is deformed to form a crater cavity structure. After the crater size reaches the maximum, it begins to contract inward, and a jet structure appears at the bottom of the crater and moves upward through the liquid level. As the jet rises to the maximum height, it collapses due to its own gravity and finally returns to the target liquid. Here, we mainly focused on the factors affecting the formation of crater and jet from the perspective of energy conservation and transformation.

Droplet impact behaviors have been classified into three stages; impact, cavity, and jet. The total energy during the collision can be written as

$$E = \frac{1}{2}Mv^2 = \frac{\pi}{12}\rho D^3 v^2 = \frac{\pi}{12}\sigma D^2 We. \tag{1}$$

According to the Refs. [30,32,35,39], at the cavity stage, the crater energy E_c is defined as

$$E_c = E_{g-c} + E_{s-c}, \tag{2}$$

where E_{g-c} is the gravitational potential energy of the cavity and E_{s-c} is the surface energy. E_{g-c} and E_{s-c} are expressed by

$$E_{g-c} = \int \rho g H_d \, dV, \tag{3}$$

$$E_{s-c} = \sigma_0 \pi H_d^2, \tag{4}$$

where σ_0 is the surface tension of the fuel. According to the Refs. [29,40]. At the jet stage, the jet energy is defined as

$$E_j = \frac{\pi}{8}\rho g d_j^2 H_j^2 + \pi d_j \left[\left(\frac{d_j}{4}\right) + H_j\right]\sigma, \tag{5}$$

where d_j is the maximum jet width and H_j is the maximum jet height. The energy conservation of impact process is computed as

$$E = E_c + E_{c^*} = E_j + E_{j^*}, \tag{6}$$

where E_{c^*} is the dissipated crater energy and E_{j^*} is dissipated jet energy. The energy of the collision process with the oil pool temperature of 50 °C, 70 °C, 90 °C, 110 °C, and 130 °C were calculated. The relationship between impact energy, crater energy and jet energy are shown in Figs. 7 and 8. The energy change trend is consistent with that by Xu *et al.*[35] Figure 7 shows the relationship between crater energy and initial impact energy E at different temperatures. When the droplet impinges on the liquid surface, part of the initial impact energy can be converted into crater energy, while the rest can be converted into waste forms such as dissipated viscosity, impingement sound energy, and wave-swell energy. This shows that as the impact energy increases, the crater energy increases. The relationship between E_c and E is nearly linear, and the regression coefficient of the fitted curve is above 99% at all temperatures. In the oil temperature range of 50 °C–130 °C, the corresponding energy conversion ratio is 31.8%–59.1%. This indicates that the energy conversion rate increases with the increase of oil temperature. The main reason is that as the temperature of the target liquid increases, the surface tension, viscous force, and density of the target liquid decrease, and other lost energy (dissipated viscous energy, wave-swell energy, and so on) decreases. Figure 8 shows the relationship between jet energy and initial impact energy at different temperatures. The jet energy increases with the increase of impact energy, because the maximum jet height increases with the increase of Weber number. The results show that E_j increases linearly with temperature, and the coefficient of fitting curve is larger than 97% at each temperature. When the oil temperature is 70 °C–130 °C, the corresponding energy conversion increases from 13.6% to 32.5% (no jet phenomenon can be observed when the oil temperature is 50 °C). This indicates that the increase of oil pool temperature is beneficial to the increase of jet scale.

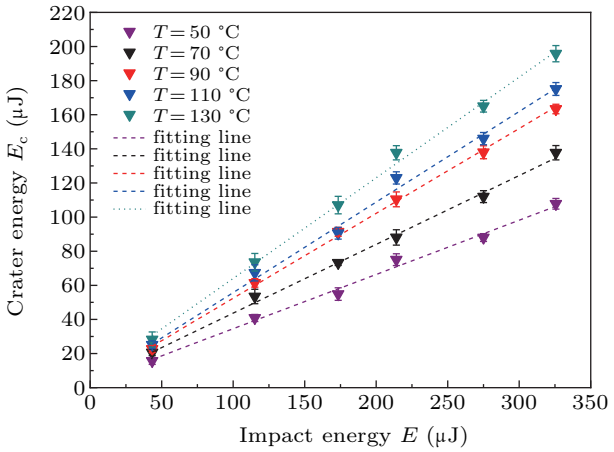


Fig. 7. The energy of the crater as a function of droplet initial impact energy.

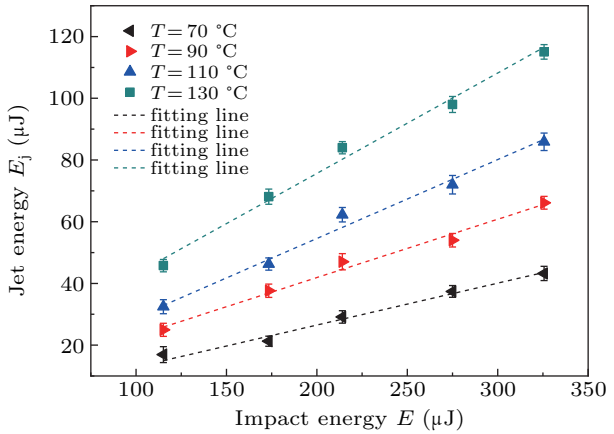


Fig. 8. The energy of the jet as a function of droplet initial impact energy.

For energy conversion in the crater-jet process, energy ratios of E_c/E and E_j/E, where E_c/E is the ratio of total energy to crater energy and E_j/E is the ratio of total energy

to jet energy, are calculated as shown in Table 3. It can be found that there is an obvious correlation between oil pool temperature and energy conversion rate. The variation of energy conversion rate with dimensionless temperature is shown in Figs. 9 and 10. The energy conversion rate is also linearly related to the dimensionless pool temperature. The correlation $E_c/E = 0.876(T_0 - T_\infty)/(T_{\text{boiling}}g - T_\infty) + 0.232$ and $E_j/E = 0.823(T_0 - T_\infty)/(T_{\text{boiling}} - T_\infty) - 0.0267$ is obtained. This provides a reference for the energy conversion ratio at different oil temperature conditions. It can be seen that the energy conversion rate is mainly related to the temperature of oil and the solubility of droplet and oil. The conversion rate increases with the increase of temperature. The reason is that with the increase of temperature, the physical properties of the oil decrease, including density, viscosity, and surface tension. With the oil temperature is 50 °C–130 °C, the density decreases from 854.5 kg/m^3 to 791.7 kg/m^3, surface tension decreases from 26.9 mN/m to 19.3 mN/m and viscosity decreases from 120.9 mPa·s to 5.1 mPa·s. It means that the resistance and viscous dissipation of the droplet impinging the oil surface decrease. Compared with the droplet impact on water,[32,41] it can be predicted that the energy conversion rate of droplet impact oil is far lower than that of droplet impact water at room temperature ($\theta = 0$) by the fitting formula of energy conversion rate and dimensionless temperature. In addition, compared with the data of Xu *et al.*,[35] the energy ratio growth of engine oil was more sensitive to dimensionless temperature than for energy ratio growth of ethanol.

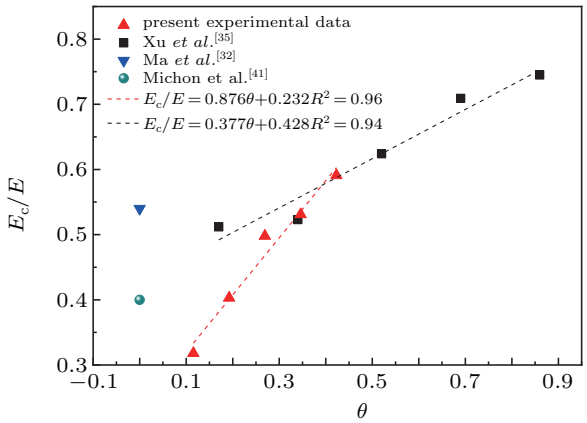


Fig. 9. The ratio of crater energy to the initial impact energy as a function of the dimensionless pool temperature.

As the oil temperature increases, the viscosity, surface tension, and density of the impact target liquid all decrease. When the droplet touches the hot oil surface, part of the initial total energy (E) is absorbed by the impact target liquid and converted into crater energy. The smaller the surface tension, viscosity, and density of the liquid are, the smaller the energy dissipation is, the more crater energy is absorbed by the target impacting the liquid, and the energy conversion ratio increases. Compared to previous studies on miscible liquid,[29,35] when the droplet touches the miscible liquid, the miscible liquid surface is easier to deform around the impact point than the immiscible liquid surface, and the energy conversion ratios of the two are also different during impact. Table 4 shows a comparison of the energy conversion ratio (E_c/E and E_j/E) between the present calculated data and those in literature studies[32,35,41,42] focusing on the interaction between droplet and miscible liquid. Pumphrey *et al.*[42] assumed that the impact energy of droplet impacting on the same liquid surface can all be converted into crater energy, regardless of energy loss, which leads to prediction deviation. Michon *et al.*[41] indicated that the energy conversion ratio is about 0.4 at room temperature. Ma *et al.*[32] presented that the value of E_c/E is around 0.54 and E_j/E is around 0.248 for the impact weber number of 204 to 640. However, Michon *et al.*[41] only calculated E_c/E without further calculating the conversion ratios of E_j/E, and the studies by Michon *et al.*[41] and Ma *et al.*[32] were carried out at room temperature, and the influence of oil temperature on the energy conversion in the impact process was not presented. Xu *et al.*[35] reported that, for droplet impacting on the ethanol liquid surface with different oil temperature, the value of E_c/E ranges from 0.512 to 0.745 and E_j/E is from 0.159 to 0.535, which are higher than those calculated in the present work. In other words, there is more energy loss when the droplet impacts on the immiscible liquid.

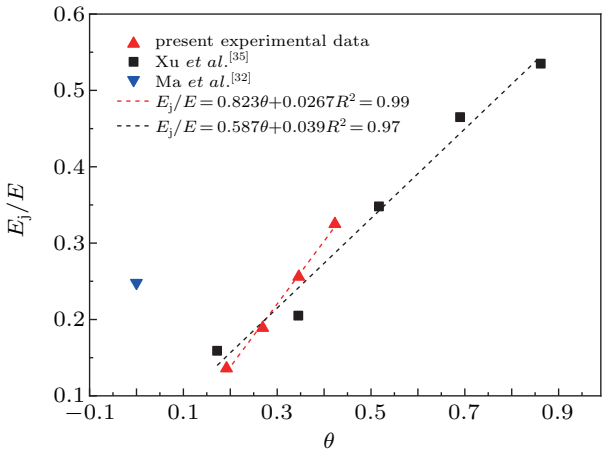


Fig. 10. The ratio of jet energy to the initial impact energy as a function of the dimensionless pool temperature.

Table 3. Energy ratios of E_c/E and E_j/E for temperatures of 50 °C, 70 °C, 90 °C, 110 °C, and 130 °C.

Energy ratio	$T = 50$ °C	$T = 70$ °C	$T = 90$ °C	$T = 110$ °C	$T = 130$ °C
E_c/E	0.318	0.403	0.498	0.531	0.591
E_j/E	-	0.136	0.189	0.256	0.325

Table 4. Comparison of energy conversion ratio (E_c/E and E_j/E) among present experimental data and those in literature studies.[32,35,41,42]

Experiments	Target liquid	Condition	E_c/E	E_j/E
Present	engine oil	50 °C–130 °C	0.318–0.590	0.136–0.325
Xu *et al.*[35]	ethanol	30 °C–70 °C	0.512–0.745	0.159–0.535
Michon *et al.*[41]	water	room temperature	around 0.40	–
Pumphrey *et al.*[42]	water	room temperature	1	–
Ma *et al.*[32]	water	room temperature	around 0.54	around 0.248

4. Conclusion

In this work, the experiments were carried out to study the influence of the liquid temperature on the interaction behavior for single water droplet impinging on the immiscible liquid. The impact Weber number and oil temperature have significant influences on the impact behaviors. For different Weber numbers and oil temperatures, three kinds of impact phenomena, including penetration, craterjet, and crater-jet–secondary jet were found. As the impact Weber number and the oil temperature increase, the maximum crater volume increases. The maximum jet height is also related to the oil temperature and the impact Weber number. Based on the analysis of the energy transfer at the three stages of the impact behavior (impact, cavity and jet), it is theoretically found that the formations of the crater and the jet structure are related to the oil temperature, fuel physical properties, impact Weber number, droplet size, *etc*. The increase of oil temperature is beneficial to improve the energy conversion ratio.

References

[1] Liang G and Mudawar I 2017 *Int. J. Heat Mass Transfer* **115** 1174
[2] Hu H B, Huang S H and Chen L B 2013 *Chin. Phys. B* **22** 084702
[3] Fan X J, Wang C J, Wang X, Li M H and Shen Z H 2019 *European Journal of Mechanics B-Fluids* **74** 191
[4] Gao X, Kong L, Li R and Han J 2017 *Int. J. Heat Mass Transfer* **108** 1068
[5] AL Y 2006 *Ann. Rev. Fluid Mech.* **38** 159
[6] Wang Z G, Wang X S, Zhu P, Chen P P, Zhao X D and Zhang H P 2017 *Journal of Loss Prevention in the Process Industries* **49** 839
[7] Gao X and Li R 2014 *Aiche Journal* **60** 2683
[8] Xu M J, Wang C J and Lu S X 2016 *Experimental Thermal and Fluid Science* **74** 347
[9] Sikalo S and Ganic E N 2006 *Experimental Thermal and Fluid Science* **31** 97
[10] Gao X and Li R 2015 *Phys. Rev. E* **92** 053005
[11] Cossali G E, Marengo M and Santini M 2008 *Int. J. Heat Fluid Flow* **29** 167
[12] An-Bang W and Chi-Chang C 2000 *Phys. Fluids* **12** 2155
[13] Sun Z H and Han R J 2008 *Chin. Phys. B* **17** 3185
[14] Fan X J, Wang C J, Guo F P, Chen B and Li M H 2021 *Int. J. Therm. Sci.* **159** 106601
[15] Visaria M and Mudawar I 2009 *IEEE Transactions on Components and Packaging Technologies* **32** 784
[16] Rein M 1993 *Fluid Dyn. Res.* **12** 61
[17] Xu M, Zhang J, Wu C, Li C, Chen X and Lu S 2018 *Acta Mechanica* **229** 1567
[18] Cong B H and Liao G X 2009 *Journal of Fire Sciences* **27** 101
[19] Worthington A M 1877 *Proc. R. Soc. Lond.* **25** 498
[20] Manzello S L, Yang J C and Cleary T G 2003 *Fire Safety Journal* **38** 651
[21] Rodriguez F and Mesler R 1985 *Journal of Colloid and Interface Science* **106** 347
[22] Liu J, Vu H, Yoon S S, Jepsen R and Aguilar G 2010 *Atomization and Sprays* **20** 297
[23] Liang G T, Guo Y L, Yang Y, Zhen N and Shen S Q 2013 *Acta Mechanica* **224** 2993
[24] Liang G T, Guo Y L, Shen S Q and Yu H 2014 *Acta Mechanica* **225** 3353
[25] Liang G T, Guo Y L, Yang Y, Guo S and Shen S Q 2013 *Experimental Thermal and Fluid Science* **51** 18
[26] Zou J, Wang P F, Zhang T R, Fu X and Ruan X D 2011 *Phys. Fluids* **23** 044101
[27] Zou J, Ren Y, Ji C, Ruan X and Fu X 2013 *Experimental Thermal and Fluid Science* **51** 332
[28] Fan X, Wang C, Li M, Chen B, Wang X and Zhang A 2018 *European Journal of Mechanics B-Fluids* **72** 144
[29] Hasegawa K and Nara T 2019 *Aip Advances* **9** 085218
[30] Xu M, Zhang J, Wu C, Li C, Chen X and Lu S 2017 *Industrial & Engineering Chemistry Research* **56** 14686
[31] Zou J, Ji C, Yuan B, Ren Y, Ruan X and Fu X 2012 *Phys. Fluids* **24** 057101
[32] Ma H, Liu C, Li X, Huang H and Dong J 2019 *Phys. Fluids* **31** 62108
[33] Stow C D and Hadfield M G 1981 *Proc. R. Soc. Lond. A* **373** 419
[34] Rioboo R, Marengo M and Tropea C 2002 *Experiments in Fluids* **33** 112
[35] Xu M J, Li C H, Wu C P, Chen X and Lu S X 2018 *Int. J. Heat Mass Transfer* **116** 817
[36] Manzello S L and Yang J C 2003 *Phys. Fluids* **15** 257
[37] Mutchler C K and Hansen L M 1970 *Science* **169** 1311
[38] Xu M, Zhang J, Li Q and Lu S 2018 *Int. J. Heat Mass Transfer* **127** 677
[39] Fedorchenko A I and Wang A B 2004 *Phys. Fluids* **16** 1349
[40] Li H, Mei S, Wang L, Gao Y and Liu J 2014 *International Journal of Heat and Fluid Flow* **47** 1
[41] Michon G J, Josserand C and Seon T 2017 *Phys. Rev. Fluids* **2** 023601
[42] Pumphrey H C and Elmore P A 1990 *Journal of Fluid Mechanics* **220** 539